TECHNICAL MEMORANDUM

283

# A two-time-level semi-Lagrangian global spectral model

C. Temperton, M. Hortal and A. Simmons

Research Department

July 1999



European Centre for Medium-Range Weather Forecasts
Europäisches Zentrum für mittelfristige Wettervorhersage
Centre européen pour les prévisions météorologiques à moyen

# A two-time-level semi-Lagrangian global spectral model

**Clive Temperton, Mariano Hortal and Adrian Simmons**

European Centre for Medium-Range Weather Forecasts, U.K.

### Summary

A three-time-level semi-Lagrangian global spectral model was introduced operationally at ECMWF in 1991. This paper first documents some later refinements to the three-time-level scheme, and then describes its conversion to a two-time-level scheme. Experimental results are presented to show that the two-time-level scheme maintains the accuracy of its three-time-level predecessor, while being considerably more computationally efficient.

**Keywords:** Two-time-level scheme; Semi-Lagrangian scheme; Spectral model.

## 1. Introduction

Semi-Lagrangian semi-implicit integration schemes, first proposed by *Robert* (1981,1982), are now well-established in numerical weather prediction models. At the European Centre for Medium-Range Weather Forecasts (ECMWF), a three-time-level semi-Lagrangian version of the forecast model was implemented operationally in 1991. *Ritchie et al.* (1995, henceforth R95) documented the semi-Lagrangian formulation of this model, and demonstrated that it was several times more efficient than its Eulerian counterpart.

In principle, a two-time-level semi-Lagrangian scheme provides a further doubling of efficiency, through a procedure which is usually referred to as "doubling the timestep". This is slightly misleading, as in a three-time-level leapfrog scheme the length of each timestep in the usual notation is $2\Delta t$, but successive timesteps overlap by $\Delta t$. More precisely, the two-time-level scheme doubles the efficiency by eliminating this overlapping, so that only half the number of timesteps is needed to complete the forecast. Viewed in this light, it is clear that the time truncation error can be the same for a three-time-level scheme and for the corresponding two-time-level scheme with a "doubled" timestep. For a two-time-level scheme to be accurate as well as efficient, it is important that second-order accuracy in time be maintained in the trajectory calculations. A simple way to achieve this was independently suggested by *McDonald and Bates* (1987) and *Temperton and Staniforth* (1987), and formed the basis for later developments.

*McDonald and Haugen* (1992, 1993) described a two-time-level semi-Lagrangian limited-area model; subsequently, *Gustafsson and McDonald* (1996) presented a comparison between spectral and finite-difference versions of this model. Recent applications of two-time-level semi-Lagrangian schemes to global finite-difference medium-range forecast models have been described by *Chen and Bates* (1996) and *Moorthi* (1997). *Côté et al.* (1998a, 1998b) describe a multi-purpose variable-resolution global finite-element model based on a two-time-level semi-Lagrangian scheme, while *Qian et al.* (1998) incorporate a two-time-level scheme in a global nonhydrostatic model.

In this paper, a two-time-level reformulation of the semi-Lagrangian global spectral model documented in R95 is presented. This two-time-level scheme was used in the operational ECMWF forecast model from December 1996 until April 1998. First, Section 2 describes some modifications to the three-time-level scheme which

were implemented during its operational lifetime. The conversion to a two-time-level scheme is then described in Section 3. Experimental results are presented in Section 4, followed by concluding remarks in Section 5. A new version of the two-time-level scheme, which was introduced operationally in 1998, is described elsewhere (*Hortal* 1999).

## 2. Modifications to the three-time-level scheme

### 2.1 General

As mentioned in R95, if the spectral variable is chosen to be virtual temperature $T_v$ rather than temperature $T$, then in a semi-Lagrangian model there is never any need to transform the moisture field $q$ to spectral space. This "gridpoint $q$" option was implemented, and horizontal diffusion of moisture (formerly done in spectral space) was switched off.

In the reduced Gaussian grid (*Hortal and Simmons* 1991), the numbers of points in latitude rows close to the poles were increased following the recommendations of *Courtier and Naughton* (1994).

### 2.2 Interpolation and averaging

Two versions of the three-time-level scheme were described in R95, differing in their treatment of vertical advection. The original "fully interpolating" version (operational from 1991 to 1992) used a complete three-dimensional semi-Lagrangian treatment of advection. Following problems of excessive eddy kinetic energy and disappointing forecast scores, this scheme was replaced by a "vertically non-interpolating" version (operational from 1992 to 1995) in which the treatment of vertical advection is in practice Eulerian except in regions of strong vertical velocity.

Subsequent developments permitted a return to the fully interpolating version. First, all "right-hand-side" terms in the dynamical equations were averaged along the trajectory as recommended by *Tanguay et al.* (1992); previously this had been done only for the momentum equations. Second, these right-hand-side terms were interpolated to the departure point of the trajectory using *linear* (instead of cubic) interpolation. For the interpolation of the advected variables themselves to the departure point it is important to retain cubic interpolation, but this was supplemented by a quasi-monotone limiter based on the ideas of *Bermejo and Staniforth* (1992). The limiter is applied in all three dimensions for the moisture field, but only in the two horizontal dimensions for the other variables. In practice, the limiter is applied in each dimension in turn as the cubic interpolation algorithm proceeds, rather than in two or three dimensions simultaneously.

With these three modifications, a fully-interpolating three-time-level semi-Lagrangian scheme was reintroduced operationally in April 1995 and used until December 1996, when it was replaced by the two-time-level scheme described in Section 3.

At this point, it is convenient to summarize the three-time-level semi-Lagrangian discretization. If the right-hand-side terms are averaged along the trajectory as described above, and if the "semi-implicit correction" terms are discretized as in Eq. (3.4) of R95 with the semi-implicit parameter $\beta$ set to its usual value of 1, then the linear contributions to the right-hand side at the central time-level $t$ cancel exactly. Each of the discretized model equations can then be written compactly as:

$$\frac{X_A^+ - X_D^-}{2\Delta t} = \frac{1}{2}(L_D^- + L_A^+) + \frac{1}{2}(N_D^0 + N_A^0) \tag{1}$$

where

$X_A^+ = X(\underset{\sim}{x}, t + \Delta t)$ is the value at the "arrival" gridpoint at $(t + \Delta t)$;

$X_D^- = X(\underset{\sim}{x} - 2\underset{\sim}{\alpha}, t - \Delta t)$ is the value interpolated at the "departure" point at $(t - \Delta t)$;

$L_A^+$ and $L_D^-$ are the linear terms defined similarly;

$N^0 = N(t)$ are the nonlinear terms, evaluated at time $t$ and averaged between the arrival and departure points.

The departure point $(\underset{\sim}{x} - 2\underset{\sim}{\alpha})$ is found by iterative solution of the (three-dimensional) displacement equation

$$2\underset{\sim}{\alpha} = 2\Delta t \underset{\sim}{V}(\underset{\sim}{x} - \underset{\sim}{\alpha}, t) \tag{2}$$

where $\underset{\sim}{V}$ is the three-dimensional wind field. The first-guess solution for Eq. (2) is given by

$$2\underset{\sim}{\alpha}^{(0)} = 2\Delta t \underset{\sim}{V}(\underset{\sim}{x}, t) \tag{3}$$

while subsequent iterations are given by

$$2\underset{\sim}{\alpha}^{(k+1)} = 2\Delta t \underset{\sim}{V}(\underset{\sim}{x} - \underset{\sim}{\alpha}^{(k)}, t). \tag{4}$$

Interpolations are performed using a (simplified) Lagrange cubic scheme including quasi-monotone limiters for the advected quantities $X_D^-$, but linearly for all other terms.

In the formulation documented in R95, $X$ represented any of the basic variables $\underset{\sim}{v}_H$ (horizontal wind vector), $T$ (temperature), $q$ (moisture) and $\ln p_s$ (log of surface pressure). Below, more recent developments are described which have modified all but the moisture equation.

### 2.3 Modified semi-Lagrangian equations

(a) *Momentum equations*

The momentum equations are treated in vector form as in R95. Following *Rochas* (1990) and *Temperton* (1997), the Coriolis terms can be incorporated in the semi-Lagrangian advection. Thus, the advected variable becomes $\underset{\sim}{v}_H + 2\underset{\sim}{\Omega} \times \underset{\sim}{r}$ where $\underset{\sim}{\Omega}$ is the earth's rotation and $\underset{\sim}{r}$ is the radial position vector, while the Coriolis terms are dropped from the right-hand side. As described by *Temperton* (1997), this reformulation is beneficial provided that the spherical geometry is treated accurately in determining the departure point and in rotating the vectors to account for the change in the orientation of the coordinate system as the particle follows the trajectory.

The discretization of the momentum equations in the notation of Eq. (1) is then:

$$X = \underset{\sim}{v}_H + 2\underset{\sim}{\Omega} \times \underset{\sim}{r}$$

$$L = -\underset{\sim}{\nabla}(\underline{\gamma} T_v + R_d T_r \ln p_s);$$

$$N = -(\underset{\sim}{\nabla}\phi + R_d T_v \underset{\sim}{\nabla} \ln p) - L$$

where $R_d$ is the gas constant for dry air, $T_r$ is a reference temperature, $\phi$ is geopotential and $\underline{\gamma}$ is the linearized hydrostatic integration matrix defined in Eq. (2.32) of R95.

In component form, $2\underset{\sim}{\Omega} \times \underset{\sim}{r}$ is just $(2\Omega a \cos\theta, 0)$ where $a$ is the earth's radius and $\theta$ is latitude. Since the latitude of the departure point is known, the term $2\underset{\sim}{\Omega} \times \underset{\sim}{r}$ in the advected variable $X$ is computed analytically rather than interpolated. An alternative semi-implicit treatment of the Coriolis terms has also been developed (*Temperton* 1997).

(b) *Continuity equation*

Modelling flow over mountains with a semi-Lagrangian integration scheme can lead to problems in the form of a spurious resonant response to steady orographic forcing. The mechanism was clarified by *Rivest et al.* (1994). Strictly speaking, the problem has little to do with the semi-Lagrangian scheme itself; rather, it is a result of the long timesteps permitted by the scheme, such that the Courant number becomes greater than 1. Recently, *Ritchie and Tanguay* (1996) proposed a modification to the semi-Lagrangian scheme which alleviates the problem. It turned out that their suggestion was easy to implement in the ECMWF model, and had additional benefits besides improving the forecast of flow over orography.

Although Ritchie and Tanguay start by introducing a change of variables in the semi-implicit time discretization, this is not necessary and a slightly different derivation is presented here. The continuity equation is written in the form

$$\frac{d}{dt}(\ln p_s) = [RHS] \tag{5}$$

where $[RHS]$ represents right-hand-side terms. The total derivative on the left-hand side is discretized in a semi-Lagrangian fashion, and the final form of the discretized equation involves a vertical summation [see Eq. (3.23) of R95].

Now split $\ln p_s$ into two parts:

$$\ln p_s = l^* + l' \tag{6}$$

where the time-independent part $l^*$ depends on the underlying orography $\phi_s$:

$$l^* = (-\phi_s)/(R_d \bar{T}) \tag{7}$$

and $\bar{T}$ is a reference temperature. The choice in (7) gives

$$\nabla\phi_s + R_d\bar{T}\nabla l^* = 0$$

so that $l^*$ is (to within an additive constant) the value of $\ln p_s$ appropriate for an isothermal state at rest with underlying orography.

Using (6) and (7),

$$\frac{d}{dt}(\ln p_s) = \frac{dl'}{dt} - \left(\frac{1}{R_d\bar{T}}\underset{\sim}{v}_H \cdot \underset{\sim}{\nabla}\phi_s\right) . \tag{8}$$

The second term on the right-hand side of (8) is now seen as a kinematic forcing. Since the orography is not advected, a semi-Lagrangian discretization is inappropriate. Instead, this term is computed in an *Eulerian* manner and transferred to the right-hand side of the continuity equation (5), which becomes

$$\frac{dl'}{dt} = [RHS] + \frac{1}{R_d\bar{T}}\underset{\sim}{v}_H \cdot \underset{\sim}{\nabla}\phi_s \ . \tag{9}$$

In (9), only the advection of $l'$ is treated in a semi-Lagrangian fashion. The extra forcing term is averaged along the trajectory like the other right-hand-side terms.

In *Ritchie and Tanguay* (1996) there is a corresponding modification of the thermodynamic equation, in the original form of which they use a semi-Lagrangian discretization of $\omega (=\mathrm{d}p/\mathrm{d}t)$. In the ECMWF model this modification is not required, as an Eulerian discretization of $\omega$ is already used [see Section 3(e) of R95 for a discussion of this point].

Since the above derivation is independent of the semi-implicit scheme, the reference temperature $\bar{T}$ in (7) does not have to be the same as the semi-implicit reference temperature $T_r$. Experiments showed that the results are insensitive to the exact choice. To avoid an unnecessary dependence on the choice made for the stability of the semi-implicit scheme (see Section 3.2), we use an ICAO standard atmosphere value of 288.15K for $\bar{T}$.

In the notation of Eq. (1), the final form for the modified continuity equation is

$$X_A^+ = \sum_{j=1}^{NLEV} \Delta B_j \{X_D^- + \Delta t(L_D^- + L_A^+ + N_D^0 + N_A^0)\}$$

where $NLEV$ is the number of model levels, the constants $\Delta B_j$ (from the discrete formulation of the hybrid vertical coordinate) are defined in R95,

$$X = \ln p_s + \phi_s/(R_d\bar{T}) \ ,$$

$$L = -\frac{1}{p_s^r}\sum_{j=1}^{NLEV}(\Delta p_j^r D_j) \ ,$$

$$N = \frac{\partial X}{\partial t} + \underline{v}_H \cdot \nabla X - L \ .$$

Here the $p_j^r$ are reference pressures, $p_s^r$ is a reference surface pressure, $D$ is divergence and $\partial X/\partial t = \partial(\ln p_s)/\partial t$ is defined by Eq. (2.14) of R95.

As also noted recently by *Moorthi* (1997), the modification of the continuity equation proposed by *Ritchie and Tanguay* (1996) improves the mass conservation properties of the semi-Lagrangian scheme. This may be attributed to the fact that the new advected variable is much smoother than the original $\ln p_s$, since the influence of the underlying orography has been subtracted out; hence, the semi-Lagrangian advection is presumably more accurate. To quantify this effect, two sets of 12 10-day forecasts were run at horizontal resolution T106 with 31 levels and a timestep of 30 minutes. In the set of forecasts with the original form of the continuity equation, the average absolute change in the global mean surface pressure after 10 days was 0.59 hPa (maximum 0.95 hPa). In the set with the modified continuity equation, the average absolute change was less than 0.02 hPa (maximum 0.04 hPa).

(c) *Thermodynamic equation*

As mentioned above, the semi-Lagrangian treatment of the continuity equation is improved by changing the advected variable to a smoother quantity which is essentially independent of the underlying orography. A similar modification has been implemented in the thermodynamic equation, borrowing an idea from the treatment of horizontal diffusion. To approximate horizontal diffusion on pressure surfaces, thereby avoiding spurious warming over mountain tops in sigma or hybrid vertical coordinates, the diffused quantity is $(T - T_c)$, with

$$T_c = \left(p_s \frac{\partial p}{\partial p_s}\frac{\partial T}{\partial p}\right)_{ref} \ln p_s$$

where '$ref$' denotes a reference value which is a function only of model level. For the purposes of the semi-Lagrangian advection $\ln p_s$ is replaced by a time-independent value as in Eq. (7) above, to define a "temperature" $T_b$ which depends only on the model level and the underlying orography:

$$T_b = -\left(p_s \frac{\partial p}{\partial p_s}\frac{\partial T}{\partial p}\right)_{ref} \cdot \phi_s/(R_d \bar{T}) \ . \qquad (10)$$

The semi-Lagrangian advection is now applied to the quantity $(T - T_b)$, while a compensating expression

$$-\underline{v}_H \cdot \nabla T_b - \dot{\eta}\frac{\partial T_b}{\partial \eta}$$

appears on the right-hand side of the equation and is computed in an Eulerian fashion (note that this time it includes a vertical advection term). In the treatment of horizontal diffusion, $T_c$ is set (abruptly) to zero above a certain level. In the definition of $T_b$, this transition is smoothed in order to maintain vertical differentiability.

In the notation of Eq. (1), the thermodynamic equation can be expressed as:

$$X = T - T_b ,$$

$$L = -\underline{\tau} D ,$$

$$N = \frac{\kappa T_v \omega}{[1 + (\delta - 1)q]p} - (\underline{v}_H \cdot \nabla T_b) - \dot{\eta}\frac{\partial T_b}{\partial \eta} - L$$

where $T_b$ is given by (10), the matrix $\underline{\tau}$ is defined in Eq. (2.33) of R95 and the discretization of the first term in the expression for $N$ is defined in Eq. (2.25) of R95.

This modified treatment of the thermodynamic equation, coupled with that of the continuity equation, has resulted in a more realistic (and less noisy) appearance of the flow over mountains.

(d) *Moisture equation*

There has been no change in the moisture equation. In the notation of Eq. (1) we have simply $X = q$, $L = 0, N = 0$.

### 2.4 Changes to the physics

In addition to the modifications to the dynamics as decribed above, several major changes to the physical parametrizations were implemented. In April 1995 a prognostic cloud scheme (*Tiedtke* 1993) was introduced, based on equations for the time evolution of cloud liquid water, cloud ice and cloud fraction. These equations include (optionally) the effects of advection, which are handled by a semi-Lagrangian treatment like that for moisture.

Also in April 1995, a new parametrization of orographic blocking effects (*Lott and Miller* 1997) was introduced in conjunction with a return from "envelope" to "mean" orography.

In September 1996, a representation of soil moisture freezing was implemented (*Viterbo et al.* 1998).

## 3. Formulation of a two-time-level scheme

### 3.1 Basic formulation

Formally, the two-time-level scheme may be written in the notation of Eq. (1) as:

$$\frac{X_A^+ - X_D^-}{\Delta t} = \frac{1}{2}(L_D^- + L_A^+) + \frac{1}{2}(N_D^* + N_A^*) \tag{11}$$

where

$X_A^+ = X(\underset{\sim}{x}, t + \Delta t)$ is the value at the "arrival" gridpoint at $(t + \Delta t)$;

$X_D^- = X(\underset{\sim}{x} - \underset{\sim}{\alpha}, t)$ is the value interpolated at the "departure" point at time $t$;

$L_A^+$ and $L_D^-$ are the linear terms defined similarly;

$N^*$ are the nonlinear terms, obtained by extrapolation in time to $\left(t + \frac{1}{2}\Delta t\right)$:

$$N^* = \frac{3}{2}N(t) - \frac{1}{2}N(t - \Delta t) \ . \tag{12}$$

The displacement equation (2) becomes

$$\underset{\sim}{\alpha} = \Delta t \underset{\sim}{V}^*\left(\underset{\sim}{x} - \frac{1}{2}\underset{\sim}{\alpha}, t + \frac{1}{2}\Delta t\right) \tag{13}$$

where the three-dimensional wind field $\underset{\sim}{V}^*$ is also extrapolated in time:

$$\underset{\sim}{V}^* = \frac{3}{2}\underset{\sim}{V}(t) - \frac{1}{2}\underset{\sim}{V}(t - \Delta t) \ . \tag{14}$$

The iterative scheme and first-guess for solving (13) are exactly analogous to those for solving (2).

The choices for the variables $X$ and for the interpolation schemes remain exactly as for the three-time-level scheme.

The semi-implicit equations to be solved in spectral space have the same form as for the three-time-level scheme, except that $\Delta t$ is replaced by $\Delta t/2$.

In principle a two-time-level scheme should have no $2\Delta t$ computational mode, and the time-filtering procedure described in Section 2(f) of R95 is no longer needed.

The rest of this section discusses a number of issues which had to be addressed in order to implement this two-time-level scheme in practice.

### 3.2 Choice of reference $T$ and $p_s$ for the semi-implicit scheme

Preliminary experiments with the two-time-level scheme showed that, for stability, a higher reference temperature $T_r$ (350K) and higher reference surface pressure $p_s^r$ (1000 hPa) were required than in the corresponding three-time-level scheme (300K and 800 hPa respectively). This was subsequently confirmed by a stability analysis (*Simmons and Temperton* 1997).

Simmons and Temperton also suggested a "second-order accurate decentering" of the linear terms which (at least for the 31-level model with the highest level at 10 hPa) allows the reference temperature to be restored to 300K, the same as for the three-time-level scheme. In this variant, the linear terms on the right-hand side of (11) are replaced by

$$\frac{1}{2}(1+\xi)(L_D^- + L_A^+) - \frac{1}{2}\xi(L_D^* + L_A^*) \tag{15}$$

where the $L^*$ values are extrapolated in time to $\left(t+\frac{1}{2}\Delta t\right)$:

$$L^* = \frac{3}{2}L(t) - \frac{1}{2}L(t-\Delta t). \tag{16}$$

As far as the time discretization is concerned, (15) is equivalent to the second-order decentering proposed by *Rivest et al.* (1994) and generalized by *Côté et al.* (1995). However the spatial discretization in (15) is much more economical, since there is no need to compute an additional departure point at $(t-\Delta t)$, and no extra interpolations are required.

The discretization (15) was adopted for the two-time-level scheme in the 31-level version of the model, with a coefficient of $\xi$=0.05 together with $T_r$=300K and $p_s^r$=1000 hPa. Some experimental results concerning the choice of the value for $\xi$ are presented in Section 4.

### 3.3 Modified treatment of the Coriolis terms

One motivation for introducing the "advective" treatment of the Coriolis terms, described in Section 2.3 above, was that this approach carries over immediately to a two-time-level scheme and avoids the complication (especially in the case of a rotated coordinate system) of treating these terms semi-implicitly. On the basis of preliminary experiments at T213 with timesteps of up to 30 minutes, *Temperton* (1997) found that incorporating the Coriolis terms in the advection in a two-time-level scheme was stable, even though the advection is based on a time-extrapolated wind field.

Later experiments at T106 with timesteps of up to 60 minutes revealed that there was, after all, a mild instability. In fact, it can easily be shown that on an $f$-plane the proposed scheme is exactly equivalent to leaving the Coriolis terms on the right-hand side and extrapolating them in time, which is just what the scheme was designed to avoid. Extending this result to a $\beta$-plane, the stability analysis of *Bates et al.* (1995) becomes relevant (even though the quantity advected here is twice the angular velocity rather than the planetary vorticity as in Bates et al.).

*Bates et al.* (1995) cured the instability by advecting the planetary vorticity with a wind averaged between time $t$ and time $(t+\Delta t)$, instead of the time-extrapolated wind. Since this leads once again to a more complicated semi-implicit scheme, a simpler predictor-corrector approach has been taken here. A provisional value of all the variables (including $\underset{\sim}{v}_H$) at time $(t+\Delta t)$ is already provided by using Eq. (11) with the unknown quantities $L_A^+$ replaced by $L_A^- = L(\underset{\sim}{x},t)$; this is done in order to furnish the parametrization schemes with "provisional" dynamical tendencies. A new horizontal displacement can then be computed via one iteration of Eq. (13) with the time-extrapolated wind at the midpoint of the trajectory replaced by the average of $\underset{\sim}{v}_H^-$ at the previously computed departure point and the provisional value of $\underset{\sim}{v}_H^+$ at the arrival

gridpoint. A new departure point, based on this time-averaged wind, is thus found. Since the latitudes of the original and the new departure points are now known, it is a simple matter to recompute the contributions of the Coriolis terms to the momentum equations; no additional interpolations are needed. Further details and experimental results illustrating the benefit of this modification are presented elsewhere (*Temperton et al.*, 1999).

### 3.4 Modified displacement equation

The final modification to the two-time-level scheme represented yet another "advantage of spatial averaging" (*Tanguay et al.* 1992). It was found that noise problems were reduced if the midpoint wind in the displacement equation was replaced by an average along the trajectory: thus, (13) becomes

$$\underset{\sim}{\alpha} = \frac{1}{2}\Delta t\left\{\underset{\sim}{V}^*\left(\underset{\sim}{x}-\underset{\sim}{\alpha},t+\frac{1}{2}\Delta t\right)+\underset{\sim}{V}^*\left(\underset{\sim}{x},t+\frac{1}{2}\Delta t\right)\right\}.$$

A similar modification could be made to the corresponding three-time-level displacement equation (2).

### 3.5 Time-stepping procedure

The time-stepping procedure for the two-time-level scheme is very similar to that for the three-time-level scheme described in R95. The only significant difference lies in the contents of the "gridpoint work files" used to pass data from one timestep to the next. In the case of the three-time-level scheme the work file contained the basic variables at time $(t-\Delta t)$, together with the $(t-\Delta t)$ contributions to the semi-implicit correction terms. In the two-time-level scheme the work files contain winds at $(t-\Delta t)$ for computing $\underset{\sim}{V}^*$ via (14), nonlinear terms at $(t-\Delta t)$ to compute $N^*$ via (12), and in the case of "second-order accurate decentering", linear terms at $(t-\Delta t)$ to compute $L^*$ via (16). The quantity of information passed from one timestep to the next is in fact greater for the two-time-level scheme than for the three-time-level, invalidating the hope that a two-time-level scheme would require less memory.

The number of Legendre and Fourier transforms is unchanged in the conversion from the three-time-level scheme to its two-time-level counterpart. In the semi-implicit equations to be solved in spectral space, the only change is to replace $2\Delta t$ by $\Delta t$. As already mentioned in Section 3.1, the time-filtering procedure described in R95 is no longer required.

### 3.6 Efficiency

The computational work per timestep is almost identical for the three- and two-time-level schemes. However, the promised doubling of efficiency is not fully achieved in the forecast model since there are some expensive calculations in the radiation scheme which are performed once every three hours whatever the choice of integration procedure. Also, the amount of computation involved in postprocessing the results remains the same.

## 4. Experimental results

This section presents the results of sets of experiments designed to compare the two-time-level scheme described in Section 3 with the three-time-level scheme, and to test the impact of various parameter choices for the two-time-level scheme. Unless stated otherwise each set of experiments consists of 24 10-day forecasts, run at horizontal resolution T213 with 31 levels. Initial conditions are taken from the operational ECMWF analyses at 12UTC on the 1st and 15th of each month from December 1995 to November 1996 inclusive. Forecasts are verified against the corresponding operational analyses.

Fig. 1 compares verification scores for the 500 hPa height field over the extratropical Northern Hemisphere (north of 20° N.). The three-time-level version was run with $\Delta t$=15 min, and the two-time-level with $\Delta t$=30 min. Scores are presented here in terms of both the anomaly correlation coefficient and the root mean square error. Since the two measures were always found to give the same signal in these experiments, subsequent figures will show only the anomaly correlation coefficient (or the correlation itself in the case of vector wind scores). In this example, the two versions of the model yield essentially identical scores.

Fig. 2(a) shows the corresponding scores for the 1000 hPa height field over Europe. Here the three-time-level scheme shows a very slight advantage around Days 4-5, while the position is reversed after Day 6. In view of the smaller verification area involved, these differences may be simply due to sampling. Fig. 2(b) shows the scores for the 850 hPa temperature over the extratropical Northern Hemisphere, and Fig. 2(c) the scores for the 850 hPa vector wind field over the Tropics. In these examples, the scores are again virtually identical.

Fig. 3 again presents scores for the 500 hPa height field over the extratropical Northern Hemisphere. Here two versions of the two-time-level scheme ($\Delta t$=30 min) are compared against the three-time-level scheme ($\Delta t$=15 min). One version has the default values of the semi-implicit reference temperature ($T_r$=300K) and the second-order decentering coefficient ($\xi$=0.05) [see Section 3.2]. The other version has $T_r$=350K and $\xi$=0, i.e., it uses a warmer reference temperature instead of decentering (*Simmons and Temperton* 1997). As can be seen in Fig. 3, the choice between these two variants of the two-time-level scheme has no impact in terms of verification scores.

Fig. 4 demonstrates that the exact choice of the second-order decentering parameter $\xi$ is not critical. Again the scores are presented for the 500 hPa height field over the extratropical Northern Hemisphere, but for a smaller sample of 12 cases (from the 15th of each month). The forecasts were all run with $T_r$=300K, but with $\xi$ chosen to be 0.025, 0.05 or 0.1.

Finally, Fig. 5 illustrates the results of a set of experiments carried out at lower horizontal resolution (T106). Here the three-time-level scheme was run with $\Delta t$=30 min, while the two-time-level scheme was run with both $\Delta t$=30 min and $\Delta t$=60 min. The scores for the two-time-level version with $\Delta t$=60 min are similar to those for the three-time-level version with 30 minutes. With the timestep reduced to 30 minutes in the two-time-level version (so that the cost of the two- and three-time-level versions becomes the same) an improvement is seen in the scores beyond Day 4, resulting from the reduced temporal truncation error (in both the dynamics and the physics).

## 5. Concluding remarks

In this paper, several modifications to the three-time-level semi-Lagrangian global spectral model documented by *Ritchie et al.* (1995) have been presented, together with the subsequent conversion to a two-time-level version. Experimental results were shown to demonstrate that forecast accuracy was maintained with the "doubled" timestep of the two-time-level scheme, and hence with a considerable improvement in efficiency.

The two-time-level scheme was implemented in the operational T213 model at ECMWF in December 1996 with a timestep of $\Delta t$=30 minutes, replacing the previous three-time-level scheme which used $\Delta t$=15 minutes. The enhanced efficiency was at the same time exploited to upgrade the ensemble prediction system from 33 members at T63 with 19 levels (Eulerian) to 51 members at T159 with 31 levels (*Buizza et al.* 1998).

The T159 model used in the ensemble prediction system was the first operational implementation at ECMWF of an idea proposed by *Côté and Staniforth* (1988), whereby a semi-Lagrangian scheme in a spectral model can be coupled with a "linear" grid rather than the "quadratic" grid needed to eliminate aliasing due to the advection terms in an Eulerian model. Thus, the T159 model used the same computational grid as had previously been employed in an Eulerian T106 model.

Despite the successful results obtained in pre-operational testing, the T213 model suffered during the subsequent winter from occasional noise problems linked to the two-time-level scheme, and in order to alleviate these the timestep was later reduced to 15 minutes. These problems led eventually to a reformulation of the two-time-level scheme which is described elsewhere (*Hortal* 1999), and which in turn permitted the successful implementation in April 1998 of an operational T319 model, again using a "linear" grid as described above.

This represented the culmination of a sequence of algorithmic improvements implemented since 1991, when the then operational full-grid Eulerian spectral model (T106, 19 levels) was replaced at ECMWF. Combining the reduced Gaussian grid (*Hortal and Simmons*, 1991), the semi-Lagrangian integration scheme (*Ritchie et al.*, 1995), the two-time-level version (this paper) and the linear grid (*Côté and Staniforth*, 1988; *Hortal*, 1999) leads to a gain in efficiency on the order of a factor of 50. This gain has been of paramount importance in improving the overall capability of the operational assimilation/forecast system.

### REFERENCES

Bates, J.R., Li, Y., Brandt, A., McCormick, S.F. and Ruge, J., 1995: A global barotropic primitive equation model based on the semi-Lagrangian advection of potential vorticity. *Q. J .R. Meteorol. Soc.*, **121**, 1981-2005.

Bermejo, R. and Staniforth, A., 1992: The conversion of semi-Lagrangian advection schemes to quasi-monotone schemes. *Mon. Weather Rev.*, **120**, 2622-2632.

Buizza, R., Petroliagis, T., Palmer, T., Barkmeijer, J., Hamrud, M., Hollingsworth, A., Simmons, A. and Wedi, N., 1998: Impact of model resolution and ensemble size on the performance of an Ensemble Prediction System. *Q. J. R. Meteorol. Soc.*, **124**, 1935-1960.

Chen, M. and Bates, J.R., 1996: Forecast experiments with a global finite-difference semi-Lagrangian model. *Mon. Weather Rev.*, **124**, 1992-2007.

Côté, J. and Staniforth, A., 1988: A two-time-level semi-Lagrangian semi-implicit scheme for spectral models. *Mon. Weather Rev.*, **116**, 2003-2012.

Côté, J., Gravel, S. and Staniforth, A., 1995: A generalized family of schemes that eliminate the spurious resonant response of semi-Lagrangian schemes to orographic forcing. *Mon. Weather Rev.*, **123**, 3605-3613.

Côté, J., Gravel, S., Méthot, A., Patoine, A., Roch, M. and Staniforth, A., 1998a: The operational CMC-MRB Global Environmental Multiscale (GEM) Model. Part I: Design considerations and formulation. *Mon. Weather Rev.*, **126**, 1373-1395.

Côté, J., Desmarais, J.-G., Gravel, S., Méthot, A., Patoine, A., Roch, M. and Staniforth, A., 1998b: The operational CMC-MRB Global Environmental Multiscale (GEM) Model. Part II: Results. *Mon. Weather Rev.*, **126**, 1397-1418.

Courtier, P. and Naughton, M., 1994: A pole problem in the reduced Gaussian grid. *Q. J. R. Meteorol. Soc.*, **120**, 1389-1407.

Gustafsson, N. and McDonald, A., 1996: A comparison of the HIRLAM gridpoint and spectral semi-Lagrangian models. *Mon. Weather Rev.*, **124**, 2008-2022.

Hortal, M., 1999: The development and testing of a new two-time-level semi-Lagrangian scheme (SETTLS) in the ECMWF forecast model. Submitted to *Q. J. R. Meteorol. Soc.*

Hortal, M. and Simmons, A.J., 1991: Use of reduced Gaussian grids in spectral models. *Mon. Weather Rev.*, **119**, 1057-1074.

Lott, F. and Miller, M.J., 1997: A new sub-grid scale orographic drag parametrization: its formulation and testing. *Q. J. R. Meteorol. Soc.*, **123**, 101-127.

McDonald, A. and Bates, J.R., 1987: Improving the estimate of the departure point in a two-time-level semi-Lagrangian and semi-implicit model. *Mon. Weather Rev.*, **115**, 737-739.

McDonald, A. and Haugen, J.E., 1992: A two-time-level, three-dimensional semi-Lagrangian, semi-implicit, limited-area gridpoint model of the primitive equations. *Mon. Weather Rev.*, **120**, 2603-2621.

McDonald, A. and Haugen, J.E., 1993: A two-time-level, three-dimensional semi-Lagrangian, semi-implicit, limited-area gridpoint model of the primitive equations. Part II. Extension to hybrid vertical coordinates. *Mon. Weather Rev.*, **121**, 2077-2087.

Moorthi, S., 1997: NWP experiments with a gridpoint semi-Lagrangian semi-implicit global model at NCEP. *Mon. Weather Rev.*, **125**, 74-98.

Qian, J.-H., Semazzi, F.H.M. and Scroggs, J.S., 1998: A global nonhydrostatic semi-Lagrangian atmospheric model with orography. *Mon. Weather Rev.*, **126**, 747-771.

Ritchie, H., Temperton, C., Simmons, A., Hortal, M., Davies, T., Dent, D. and Hamrud, M., 1995: Implementation of the semi-Lagrangian method in a high-resolution version of the ECMWF forecast model. *Mon. Weather Rev.*, **123**, 489-514.

Ritchie, H. and Tanguay, M., 1996: A comparison of spatially averaged Eulerian and semi-Lagrangian treatments of mountains. *Mon. Weather Rev.*, **124**, 167-181.

Rivest, C., Staniforth, A. and Robert, A., 1994: Spurious resonant response of semi-Lagrangian discretizations to orographic forcing: diagnosis and solution. *Mon. Weather Rev.*, **122**, 366-376.

Robert, A., 1981: A stable numerical integration scheme for the primitive meteorological equations. *Atmos.-Ocean*, **19**, 35-46.

Robert, A., 1982: A semi-Lagrangian and semi-implicit numerical integration scheme for the primitive meteorological equations. *J. Meteorol. Soc. Japan*, **60**, 319-325.

Rochas, M., 1990: ARPEGE Documentation, Part 2, Ch. 6 (available from Météo-France).

Simmons, A.J. and Temperton, C., 1997: Stability of a two-time-level semi-implicit integration scheme for gravity wave motion. *Mon. Weather Rev.*, **125**, 600-615.

Tanguay, M., Yakimiw, E., Ritchie, H. and Robert, A., 1992: Advantages of spatial averaging in semi-Lagrangian schemes. *Mon. Weather Rev.*, **120**, 113-123.

Temperton, C., 1997: Treatment of the Coriolis terms in semi-Lagrangian spectral models. *The André J. Robert Memorial Volume*, Canadian Meteorological and Oceanographical Society, 293-302.

Temperton, C. and Staniforth, A., 1987: An efficient two-time-level semi-Lagrangian semi-implicit integration scheme. *Q. J. R. Meteorol. Soc.*, **113**, 1025-1039.

Temperton, C., Untch, A., Jablonowski, C. and Hortal, M., 1999: Treatment of the Coriolis terms in two-time-level semi-Lagrangian models (*in preparation*).

Tiedtke, M., 1993: Representation of clouds in large-scale models. *Mon. Weather Rev.*, **121**, 3040-3060.

Viterbo, P., Beljaars, A., Mahfouf, J.-F. and Teixeira, J., 1998: The representation of soil moisture freezing and its impact on the stable boundary layer. ECMWF Research Department Technical Memorandum No. 255 [submitted to *Q. J. R. Meteorol. Soc.*].

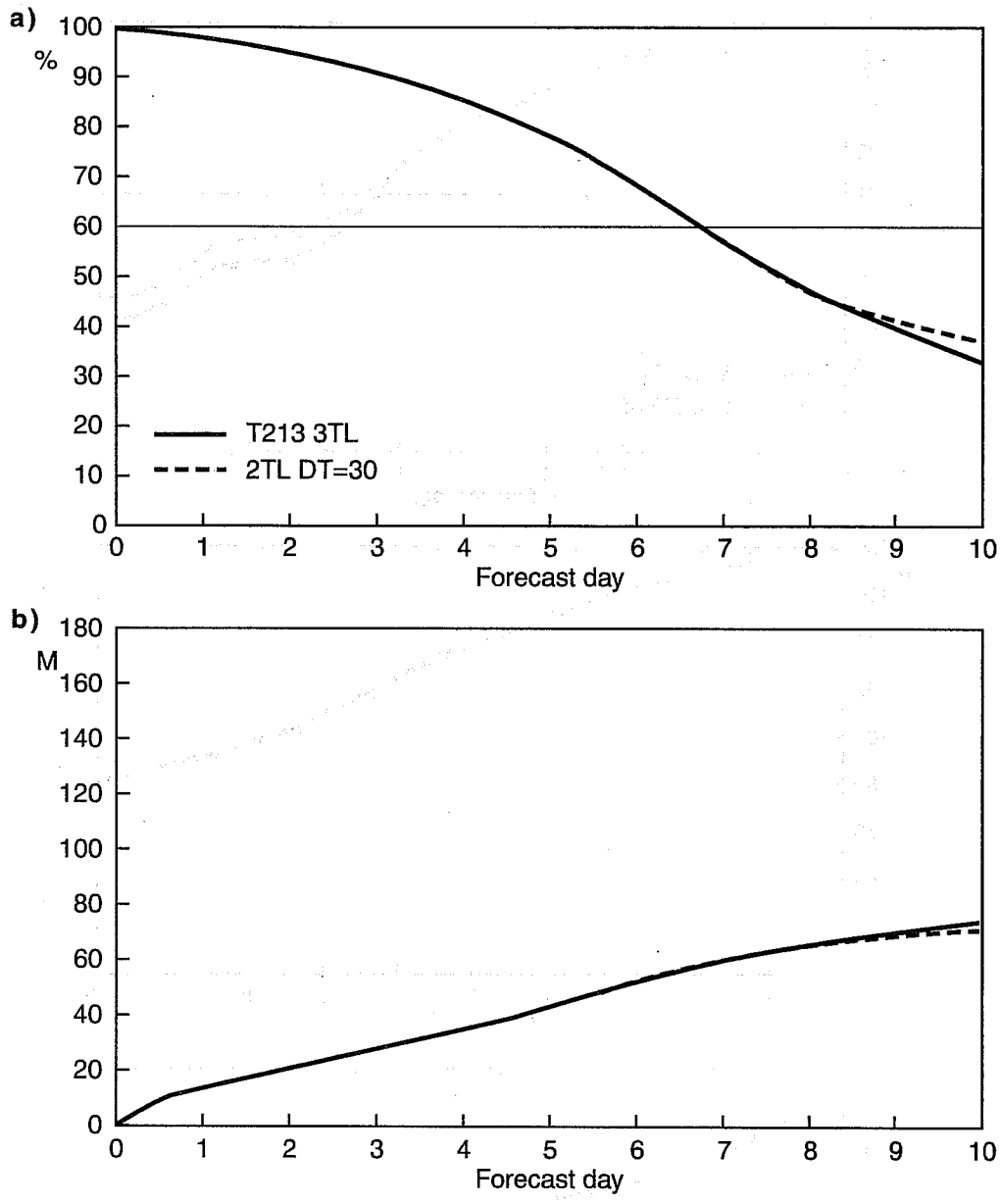


Figure 1 Verification scores for the 500 hPa height field over the extratropical Northern Hemisphere, comparing the three-time-level scheme with $\Delta t$ = 15 min (solid) and the two-time-level scheme with $\Delta t$ = 30 min (dashed): (a) anomaly correlation; (b) root mean square error.

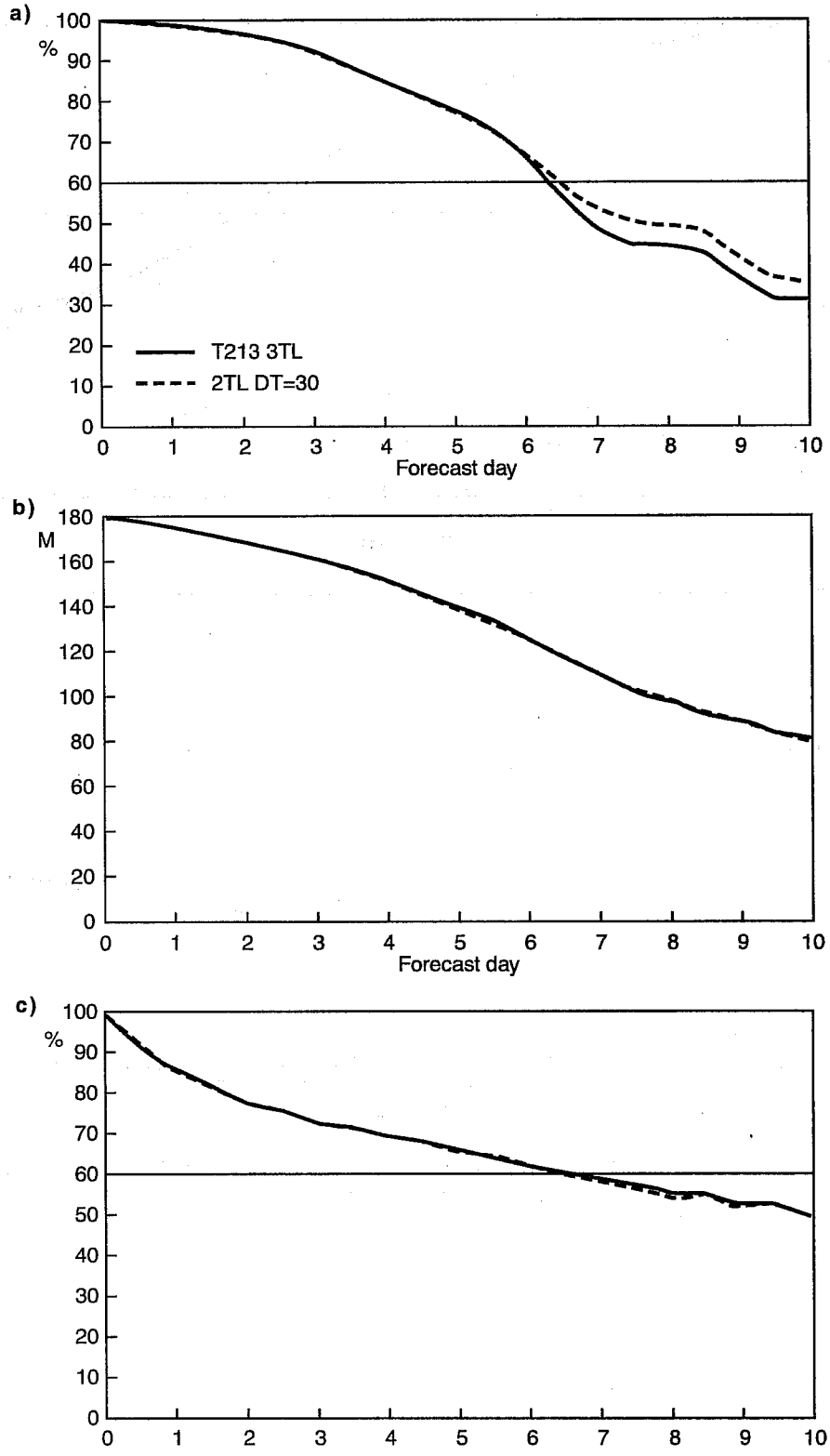


Figure 2 Verification scores, comparing the three-time-level scheme with $\Delta t$ = 15 min (solid) and the two-time-level scheme with $\Delta t$ = 30 min (dashed): (a) 1000 hPa height field over Europe; (b) 850 hPa temperature field over the extratropical Northern Hemisphere; (c) 850 hPa wind field over the Tropics.

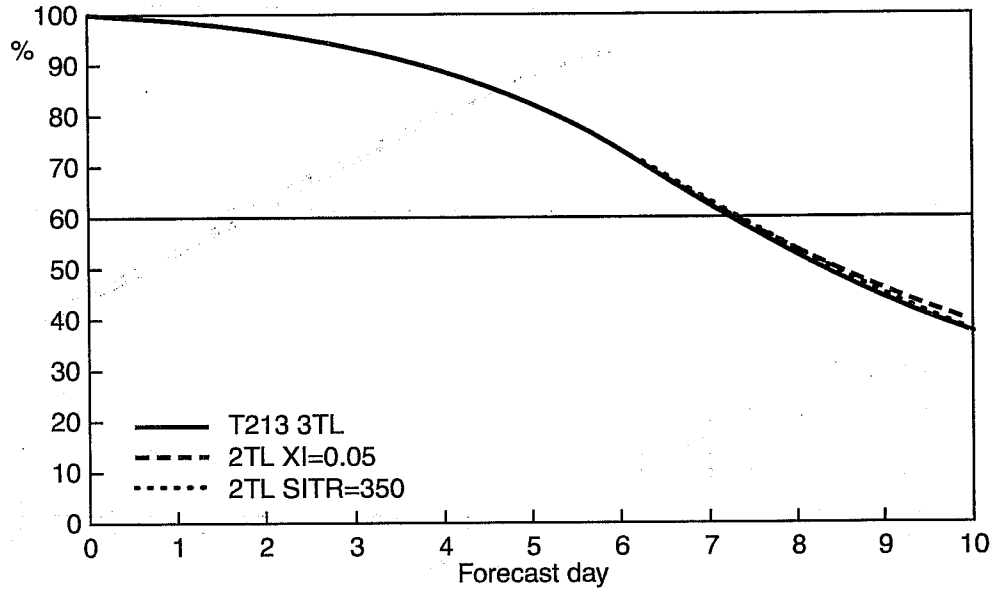


Figure 3 Verification scores for the 500 hPa height field over the extratropical Northern Hemisphere, comparing the three-time-level scheme with $\Delta t$ = 15 min (solid) and the two-time-level scheme with $\Delta t$ = 30 min: $T_r$ = 300K, $\xi$ = 0.05 (dashed) and $T_r$ = 350K, $\xi$ = 0 (dotted).

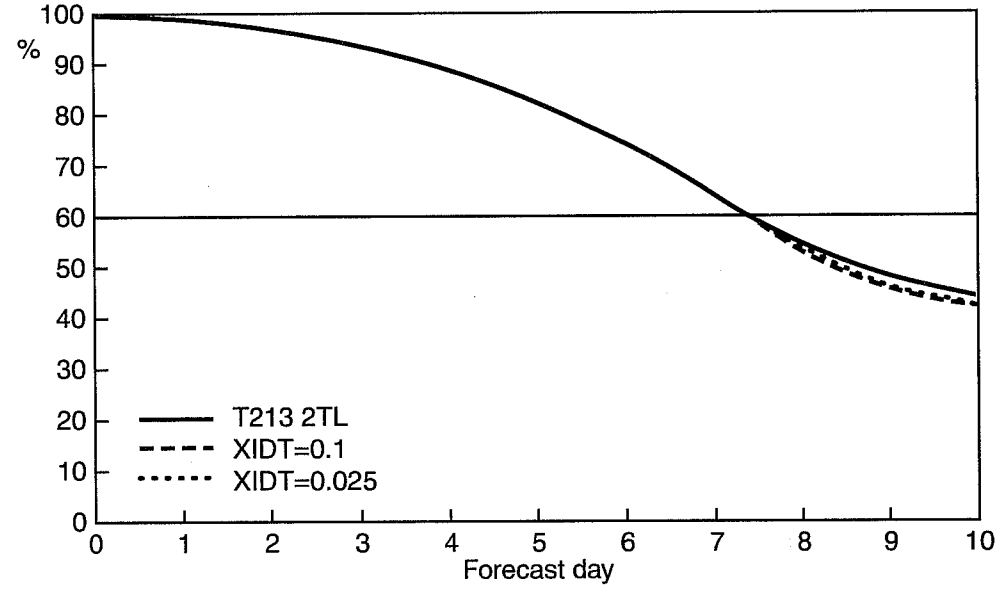


Figure 4 Verification scores for the 500 hPa height field over the extratropical Northern Hemisphere, for the two-time-level scheme with $\Delta t$ = 30 min and $T_r$ = 300K: $\xi$ = 0.05 (solid), $\xi$ = 0.1 (dashed), $\xi$ = 0.025 (dotted).

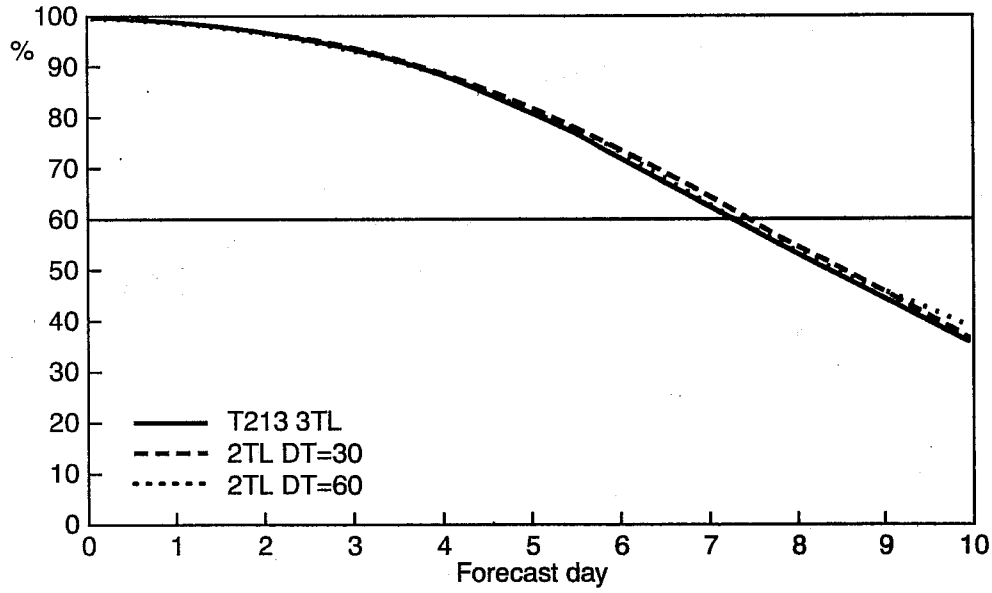


Figure 5 Verification scores for the 500 hPa height field over the extratropical Northern Hemisphere at T106, comparing the three-time-level scheme with $\Delta t$ = 30 min (solid) and the two-time-level scheme with $\Delta t$ = 30 min (dashed) and $\Delta t$ = 60 min (dotted).